Diffraction-arrested soliton self-frequency shift of few-cycle laser pulses in a photonic-crystal fiber

E. E. Serebryannikov and A. M. Zheltikov*
Physics Department, International Laser Center, M. V. Lomonosov Moscow State University, Vorob'evy gory, Moscow 119992, Russia

S. Köhler, N. Ishii, C. Y. Teisset, T. Fuji, F. Krausz,† and A. Baltuška‡
Max-Planck-Institut für Quantenoptik, Hans-Kopfermann-Strasse 1, D-85748 Garching, Germany
(Received 23 December 2005; published 19 June 2006)

The balance between diffraction and index-step guiding in photonic-crystal fibers is controlled by modifying the fiber structure, leading to different wavelength dependences of the effective mode area $S_{\text{eff}}(\lambda)$ and providing a mechanism to control nonlinear-optical phenomena. In optical fibers with a steep $S_{\text{eff}}(\lambda)$ profile, the guided mode of the light field tends to become much less compact with an increase in radiation wavelength, slowing down the Raman-induced soliton self-frequency shift of an ultrashort laser pulse. A 100-nm reduction of the soliton self-frequency shift is demonstrated for 6-fs input laser pulses.

DOI: 10.1103/PhysRevE.73.066617 PACS number(s): 42.65.Wi

I. INTRODUCTION

Dispersion limits the localization of optical waves in time, leading to the temporal spreading of optical wave packets. In waveguides, the total dispersion sensed by guided modes of the light field may substantially differ from the dispersion of waves in a bulk material. Optical waveguides of a new type—photonic-crystal fibers (PCFs) [1]—have been recently shown to provide a unique dispersion tunability, allowing dispersion properties unattainable and unthinkable for standard optical fibers to be designed through fiber structure modifications [2]. This remarkable property of PCFs has made them a powerful tool of optical technologies, allowing the creation of novel light sources [3] and frequency shifters [4] for frequency metrology [5,6], nonlinear spectroscopy [7] and microscopy [8], biomedical optics [9], and few-cycle parametric chirped-pulse amplification [10].

While dispersion is responsible for the temporal spreading of optical wave packets, diffraction limits the localization of light beams in space. In optical waveguides, diffraction is balanced by the refractive-index-step confinement of electromagnetic field, allowing a long-distance transmission of optical signals. The degree of spatial confinement of electromagnetic radiation in waveguides is quantified by the effective mode area $S_{\text{eff}}=[\int_{-\infty}^{\infty}\int_{-\infty}^{\infty}|F(x,y)|^2dx\,dy]^2/\int_{-\infty}^{\infty}\int_{-\infty}^{\infty}|F(x,y)|^4dx\,dy$, where $F(x,y)$ is the field profile in a waveguide mode. In standard optical fibers, the effective mode area is controlled by the ratio of the core diameter to the radiation wavelength and the index step from the core to the cladding. Here, we show that in PCFs, the wavelength dependence of the effective mode area $S_{\text{eff}}(\lambda)$ can be engineered by modifying the geometry of the fiber. We will demonstrate below in this paper that these changes in the diffraction-induced wavelength dependence of the effective mode area can lead to dramatic changes in the scenarios of nonlinear-optical interactions of few-cycle laser pulses in PCFs, offering ways to control spectral transformations of ultrashort pulses in PCFs through $S_{\text{eff}}(\lambda)$ tailoring.

II. BASIC EQUATIONS AND MODELING

We start with the analysis of $S_{\text{eff}}(\lambda)$ profiles for two types of PCFs. Fibers of the first type are high-index-step silica PCFs with a core diameter of 2.5 μm (the inset in Fig. 1). Fibers of the second type have a structure typical of commercial silica PCFs (e.g., the NL-PM PCF series from Crystal Fibre [11]) with a core diameter of 1.8 μm. We calculate field profiles $F(x,y)$ by using a procedure based on series expansion in localized functions [12]. The field profiles of the fundamental PCF modes are then employed to calculate the effective mode area S_{eff}. The wavelength dependence of S_{eff} for the first type of PCF is shown by curve 1 in Fig. 1. As

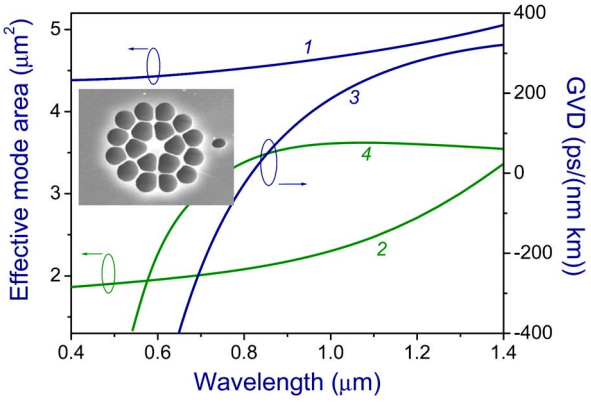

FIG. 1. (Color online) The effective mode area (1, 2) and the group-velocity dispersion (3, 4) for the PCFs of the first (1, 3) and second (2, 4) types. The inset shows a scanning electron microscopy image of the first-type PCF with a core diameter of 2.5 μm.

*Electronic address: zheltikov@phys.msu.ru
†Also at Department für Physik, Ludwig-Maximilians-Universität Munich, D-85748 Garching, Germany.
‡Electronic address: andrius.baltuska@mpq.mpg.de

the radiation wavelength changes from 0.8 to 1.4 μm (a typical wavelength shift in experiments described below in this paper), the effective mode area increases from 4.5 to 5.0 μm^2, i.e., by 11%. For PCFs of the second type, within the same range of wavelength variation, S_{eff} changes from 2.1 to 3.4 μm^2 (curve 2 in Fig. 1), i.e., by 62%. These results show that, similar to the structural dispersion tailoring, the balance between diffraction and index-step guiding in PCFs can be controlled by modifying the fiber structure, leading to substantially different $S_{\text{eff}}(\lambda)$ profiles.

We consider a soliton self-frequency shift (SSFS) [13,14] as an interesting and practically important example of a nonlinear-optical process that can be controlled through the $S_{\text{eff}}(\lambda)$ profile tailoring in PCFs. SSFS is observed for optical solitons propagating in media with noninstantaneous nonlinear response. Such solitons experience continuous frequency down-shifting due to the Raman effect [13,14]. PCFs can substantially enhance this nonlinear-optical process [15] due to a strong field confinement in a small-size fiber core and dispersion tunability. Redshifted solitons produced by sub-6-fs laser pulses in PCFs have been demonstrated to allow a synchronized seeding of a picosecond neodymium-doped yttrium aluminum garnet (Nd:YAG) pump laser, substantially simplifying few-cycle-pulse optical parametric chirped-pulse amplification [10].

To analyze the SSFS in PCFs with a frequency-dependent effective mode area, we numerically solve the generalized nonlinear Schrödinger equation (GNSE) [16], modified to include the $S_{\text{eff}}(\lambda)$ profile. In earlier related work, Mamyshev and Chernikov [17] have theoretically demonstrated that the assumption of a frequency-independent mode area leads to an overestimation of the SSFS in optical fibers. Karasawa *et al.* [18] have shown that the wavelength dependence of S_{eff} can give rise to observable effects in the waveguide spectral broadening of ultrashort laser pulses. Kibler *et al.* [19] have recently analyzed the GNSE with a wavelength-dependent mode area, demonstrating that the $S_{\text{eff}}(\lambda)$-related effects may become noticeable in spectral transformation and supercontinuum generation processes in PCFs in the regimes where the Raman effect gives rise to large SSFS.

Our numerical procedure is based on the solution of the GNSE for the field envelope $A=A(z,t)$, with the nonlinear polarization term including the retarded nonlinearity of the fiber material and the wavelength dependence of the effective mode area:

$$\frac{\partial A}{\partial \xi} = i\sum_{k=2}^{6} \frac{(i)^k}{k!}\beta^{(k)}\frac{\partial^k A}{\partial \tau^k} + P_{\text{nl}}(\xi,\tau), \tag{1}$$

where z is the propagation coordinate, t is the time variable, τ is the retarded time, and $\beta^{(k)}=\partial^k\beta/\partial\omega^k$ are the coefficients in the Taylor-series expansion of the propagation constant β. The nonlinear polarization $P_{\text{nl}}(\xi,\tau)$ in Eq. (1) is defined as

$$P_{\text{nl}}(\xi,\tau) = i\hat{F}^{-1}\left(\frac{n_2\omega}{cS_{\text{eff}}(\omega)}\tilde{p}_{\text{nl}}(\xi,\omega_0-\omega)\right), \tag{2}$$

where n_2 is the nonlinear refractive index of the fiber material, ω is the current frequency, ω_0 is the central frequency of the input field, c is the speed of light, and the operator $\hat{F}^{-1}(\cdot)$ denotes the inverse Fourier transform. The frequency-domain nonlinear polarization in Eq. (2) is defined through the direct Fourier transform

$$\tilde{p}_{\text{nl}}(\xi,\omega-\omega_0) = \hat{F}\left(A(\xi,\tau)\int_{-\infty}^{\infty} R(t)|A(\xi,\tau-t)|^2 dt\right), \tag{3}$$

including both the instantaneous, Kerr nonlinearity and the retarded, Raman contribution via the nonlinear response function

$$R(t) = (1-f_R)\delta(t) + f_R\Theta(t)\frac{\tau_1^2+\tau_2^2}{\tau_1\tau_2^2}e^{-t/\tau_2}\sin\left(\frac{t}{\tau_1}\right), \tag{4}$$

where f_R is the fractional contribution of the Raman response; $\delta(t)$ and $\Theta(t)$ are the delta and the Heaviside step functions, respectively; τ_1 and τ_2 are the characteristic times of the Raman response of the fiber material. For fused silica, $f_R=0.18$, $\tau_1=12.5$ fs, and $\tau_2=32$ fs. The nonlinear polarization $P_{\text{nl}}(\xi,\tau)$ defined in the form of Eq. (2) not only helps to include the influence of the frequency-dependent effective mode area S_{eff} on the nonlinear coefficient $\gamma=(n_2\omega)/(cS_{\text{eff}})$, but also gives a correct definition of the local field intensity, which also depends on $S_{\text{eff}}(\omega)$.

Results of numerical simulations performed with the use of Eqs. (1)–(4) for the first- and second-type PCFs are presented in Figs. 2 and 3, respectively. The spectrum of the input laser pulse in these simulations (inset in Fig. 2) corresponded to the spectrum of 6-fs pulses of a Ti:sapphire laser oscillator employed in the experiments described below. For the PCF of the first type, the wavelength dependence of the effective mode area is weak (curve 1 in Fig. 1), leading to nearly negligible (within 10%) changes in the SSFS. For the PCF of the second type, the situation is radically different. The diffraction-induced increase in the mode area in the longer-wavelength spectral region for this type of fiber (curve 2 in Fig. 1) effectively lowers the nonlinearity and reduces the field intensity for low-frequency spectral components of the radiation field. Comparison of curves 1 and 2 in Fig. 3 shows that the inclusion of the wavelength dependence of S_{eff} in Eqs. (1)–(4) reduces the SSFS in the second-type PCF with a length of 20 cm by 85 nm for the input pulse energy of 0.45 nJ [Fig. 3(a)] and by approximately 100 nm for the input pulse energy of 0.30 nJ [Fig. 3(b)].

III. EXPERIMENTAL RESULTS AND DISCUSSION

In experiments, we used a broadband chirped-mirror Ti:sapphire oscillator [20], generating 6-fs pulses with an energy up to 4 nJ at a repetition rate of 70 MHz. The laser energy coupled into PCF samples was varied from 0.1 to 2 nJ. The spectrum of laser pulses coupled into PCFs is shown in the inset to Fig. 2. To get access to the evolution of laser pulses in the process of propagation along the fiber, we measured the spectra of radiation at the output of the PCFs as a function of the fiber length. The PCF length was gradually reduced in these experiments by the destructive

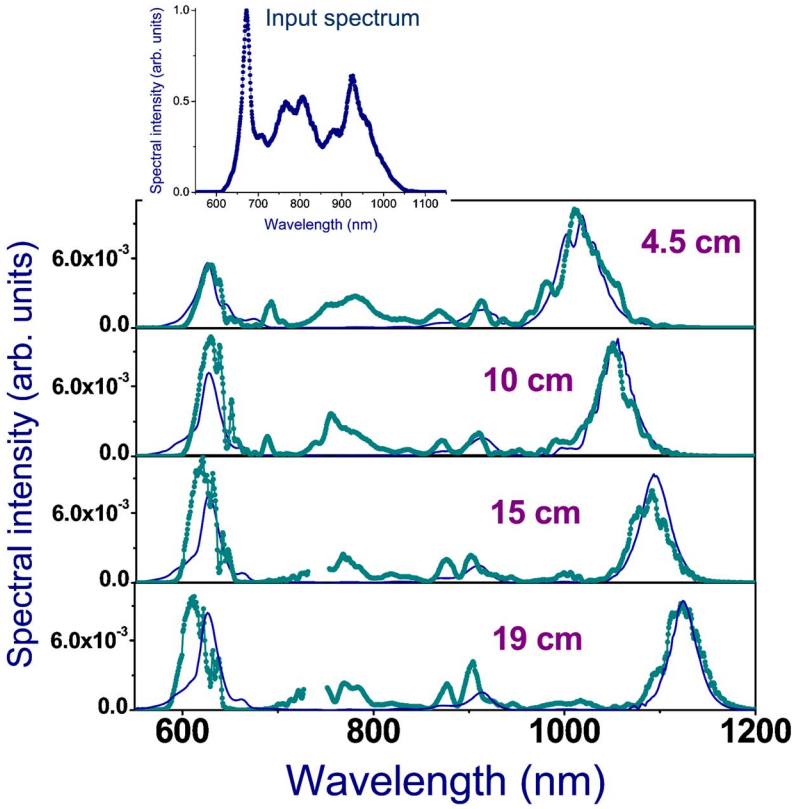

FIG. 2. (Color online) Output spectra measured (circles) and calculated (solid line) for a 2-nJ few-cycle laser pulse (the input spectrum is shown in the inset) transmitted through the first-type PCF with a variable length—from top to bottom 4.5, 10, 15, and 19 cm.

cutback approach with input pulse parameters remaining unchanged. These measurements yielded a series of PCF output spectra, visualizing the spectral transformation dynamics of few-cycle pulses in the PCF.

For the PCF of the first type, which displays a weak $S_{\text{eff}}(\lambda)$ dependence (curve 1 in Fig. 1), the main features in the experimental output spectra (Fig. 2) are adequately described by Eqs. (1)–(4) with a wavelength-independent mode area S_{eff}. In particular, the theoretical model accurately predicts the central wavelengths and the amplitudes of the redshifted solitonic components. For the PCF of the second type, GNSE simulations with a frequency-independent mode area [curves 1 in Figs. 3(a) and 3(b)] yield a substantially overestimated soliton frequency shift. As the solitonic part of the field is shifted toward longer wavelengths, the mode area S_{eff} rapidly increases (curve 2 in Fig. 1), effectively lowering the nonlinearity and reducing the field intensity for low-frequency spectral components of the radiation field in the fiber. The inclusion of the realistic $S_{\text{eff}}(\lambda)$ profile in Eqs. (1)–(4) allows the soliton frequency shift to be predicted with a rather high accuracy [cf. curves 2 and 3 in Figs. 3(a) and 3(b)]. As the increase in S_{eff} in the long-wavelength part of the spectrum slows down the SSFS, the central frequency of the soliton becomes less sensitive to variations in the input laser power. In the time domain, this corresponds to a decrease in the timing jitter of the frequency-shifted soliton induced by fluctuations in the input laser energy. This regime of SSFS in PCFs with a tailored $S_{\text{eff}}(\lambda)$ profile is therefore ideally suited for a precise spectral matching of frequency-shifted solitons with the gain band of amplifying cascades or a transmission band of filters in spectroscopic measurements, as well as for an improved temporal synchronization of Raman-shifted solitonic signals with external short-pulse laser sources.

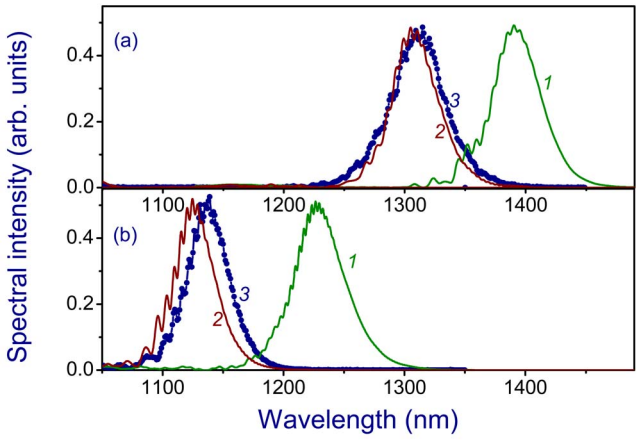

FIG. 3. (Color online) The spectral intensity of the redshifted output of the second-type PCF: (1, 2) GNSE solution with a frequency-independent effective mode area (1) and with the $S_{\text{eff}}(\lambda)$ profile shown by curve 2 in Fig. 1 (2); (3) results of experiments performed with the PCF of the second type. The spectrum of the input pulse is shown in the inset to Fig. 2. The input pulse energy is 0.45 (a) and 0.30 nJ (b).

IV. CONCLUSION

We have shown in this work that, similar to structural dispersion tailoring in PCFs, the balance between diffraction

and index-step guiding in PCFs can be controlled by modifying the fiber structure, leading to substantially different wavelength dependences of the effective mode area $S_{\mathrm{eff}}(\lambda)$. In its turn, the $S_{\mathrm{eff}}(\lambda)$ profile is shown to control the SSFS of few-cycle pulses. A 100-nm reduction of the SSFS is demonstrated for 6-fs input laser pulses.

ACKNOWLEDGMENTS

We are grateful to K. V. Dukel'skii, A. V. Khokhlov, Yu. N. Kondrat'ev, and V. S. Shevandin for fabricating fiber samples. E.E.S. and A.M.Z. acknowledge partial support of their research by the Russian Foundation for Basic Research (Projects No. 06-02-16880-a, No. 04-02-39002-GFEN2004, and No. 05-02-90566-NNS), the Russian Federal Research and Technology Program (Contract No. 02.434.11.2010), and INTAS (Projects No. 03-51-5037 and No. 03-51-5288). This project was also supported in part by the LaserLab Europe and XTRA European networks. The research described in this publication was made possible in part by Award No. RUP2-2695 of the U.S. Civilian Research & Development Foundation for the Independent States of the Former Soviet Union (CRDF).

[1] P. St. J. Russell, Science **299**, 358 (2003).
[2] W. H. Reeves, D. V. Skryabin, F. Biancalana, J. C. Knight, P. St. J. Russell, F. G. Omenetto, A. Efimov, and A. J. Taylor, Nature (London) **424**, 511 (2003).
[3] W. J. Wadsworth, A. Ortigosa-Blanch, J. C. Knight, T. A. Birks, T. P. M. Mann, and P. St. J. Russell, J. Opt. Soc. Am. B **19**, 2148 (2002).
[4] S. O. Konorov and A. M. Zheltikov, Opt. Express **11**, 2440 (2003).
[5] D. J. Jones, S. A. Diddams, J. K. Ranka, A. Stentz, R. S. Windeler, J. L. Hall, and S. T. Cundiff, Science **288**, 635 (2000).
[6] R. Holzwarth, T. Udem, T. W. Hänsch, J. C. Knight, W. J. Wadsworth, and P. St. J. Russell, Phys. Rev. Lett. **85**, 2264 (2000).
[7] S. O. Konorov, D. A. Akimov, E. E. Serebryannikov, A. A. Ivanov, M. V. Alfimov, and A. M. Zheltikov, Phys. Rev. E **70**, 057601 (2004).
[8] H. N. Paulsen, K. M. Hilligsøe, J. Thøgersen, S. R. Keiding, and J. J. Larsen, Opt. Lett. **28**, 1123 (2003).
[9] I. Hartl, X. D. Li, C. Chudoba, R. K. Rhanta, T. H. Ko, J. G. Fujimoto, J. K. Ranka, and R. S. Windeler, Opt. Lett. **26**, 608 (2001).
[10] C. Y. Teisset, N. Ishii, T. Fuji, T. Metzger, S. Köhler, R. Holzwarth, A. Baltuška, A. M. Zheltikov, and F. Krausz, Opt. Express **13**, 6550 (2005).
[11] http://www.crystal-fibre.com/
[12] T. M. Monro, D. J. Richardson, N. G. R. Broderick, and P. J. Bennet, J. Lightwave Technol. **18**, 50 (2000).
[13] F. M. Mitschke and L. F. Mollenauer, Opt. Lett. **11**, 659 (1986).
[14] E. M. Dianov, A. Ya. Karasik, P. V. Mamyshev, A. M. Prokhorov, V. N. Serkin, M. F. Stel'makh, and A. A. Fomichev, JETP Lett. **41**, 294 (1985).
[15] X. Liu, C. Xu, W. H. Knox, J. K. Chandalia, B. J. Eggleton, S. G. Kosinski, and R. S. Windeler, Opt. Lett. **26**, 358 (2001).
[16] G. P. Agrawal, *Nonlinear Fiber Optics* (Academic, San Diego, 2001).
[17] P. V. Mamyshev and S. V. Chernikov, Opt. Lett. **15**, 1076 (1990).
[18] N. Karasawa, S. Nakamura, N. Nakagawa, M. Shibata, R. Morita, H. Shigekawa, and M. Yamashita, IEEE J. Quantum Electron. **37**, 398 (2001).
[19] B. Kibler, J. M. Dudley, and S. Coen, Appl. Phys. B: Lasers Opt. **81**, 337 (2005).
[20] T. Fuji, A. Unterhuber, V. S. Yakovlev, G. Tempea, A. Stingl, F. Krausz, and W. Drexler, Appl. Phys. B: Lasers Opt. **77**, 125 (2003).